Biophysical Journal, Volume *116*

Supplemental Information

A Cholesterol Analog Induces an Oligomeric Reorganization of VDAC

Fraser G. Ferens, Trushar R. Patel, George Oriss, Deborah A. Court, and Jörg Stetefeld

A cholesterol analogue induces an oligomeric reorganization of VDAC

Fraser G. Ferens, Trushar R. Patel, George Orriss, Deborah A. Court, Jörg Stetefeld

Supplementary Information

Table S1. Raw Data obtained from AUC c(s) distributions

Detergent	Total VDAC Concentration (mg/ml)	VDAC Peak	$S_{20, buffer}$[a] (Absorbance/Interference)	A_{280}[b]	J[c]
0.3%DM	0.49	Monomer	4.53/4.57	0.40	3.29
	0.67	Monomer	4.41/4.56	0.61	5.44
	0.82	Monomer	4.38/4.52	0.72	6.33
	0.98	Monomer	4.33/4.48	0.84	7.66
0.3% DM + 0.06% CHS	0.48	Dimer	5.04/5.16	0.054	0.54
		Trimer	6.04/6.01	0.089	0.95
		Tetramer	7.19/7.35	0.229	1.83
	0.63	Dimer	5.01/5.11	0.091	0.99
		Trimer	6.07/6.01	0.172	1.38
		Tetramer	7.13/7.13	0.261	2.19
	0.84	Dimer	5/4.9	0.241	2.43
		Trimer	5.99/6.04	0.316	2.62
		Tetramer	7.08/7.06	0.179	1.34
	0.99	Dimer	4.94/ 4.84	0.414	3.89
		Trimer	5.93/ 5.95	0.319	2.75
		Tetramer	7.1/ 7.05	0.134	0.94

[a]$S_{20, buffer}$: Sedimentation coefficient of peak in sample buffer

[b]A_{280}: Absorbance at 280nm calculated by integration of species peak in the c(s) absorbance distribution

[c]J : interference fringe displacement calculated by integration of species peak in the c(s) interference distribution

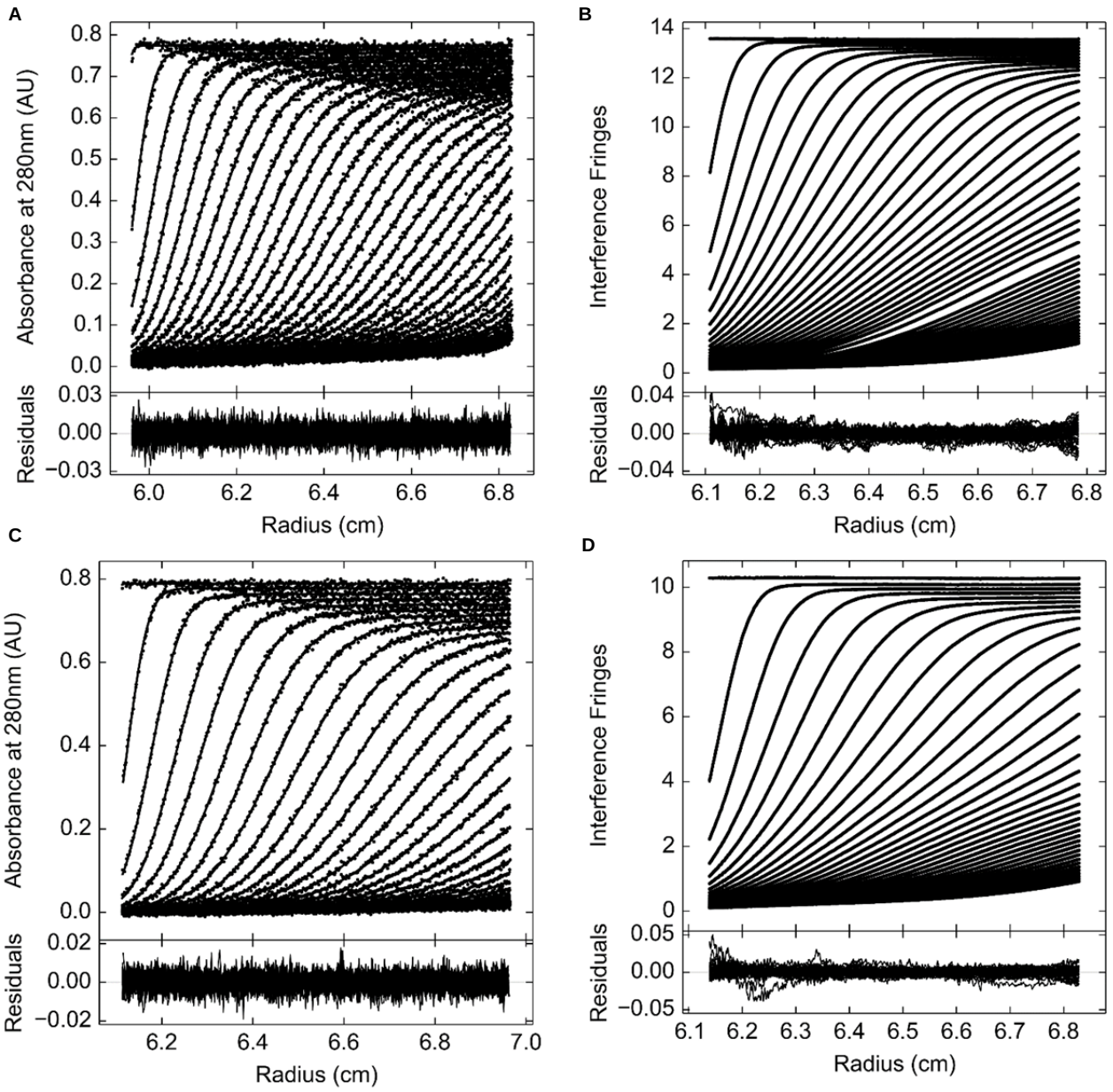

Figure S1. Representative sedimentation velocity experimental data and fitted curves used to calculate c(s) or c(s, f/f_0) distributions. (A) 0.82mg/ml $VDAC^R$ solution measured by absorbance at 280nm. (B) 0.82mg/ml VDAC in DM solution measured by interference. (C) 0.84mg/ml $VDAC^R$+CHS solution measured by absorbance at 280nm (D) 0.84mg/ml $VDAC^R$+CHS solution measured by interference. In all panels data points are presented as black circles and fitted sedimentation boundaries are depicted as black lines. For clarity only every third time point is presented.

A

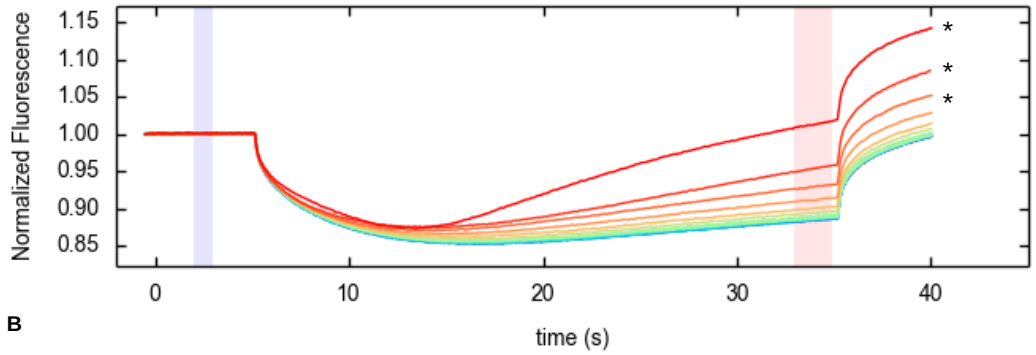
Normalized Fluorescence
1.15
1.10
1.05
1.00
0.95
0.90
0.85
0
10
20
30
40
time (s)
*
*
*

B

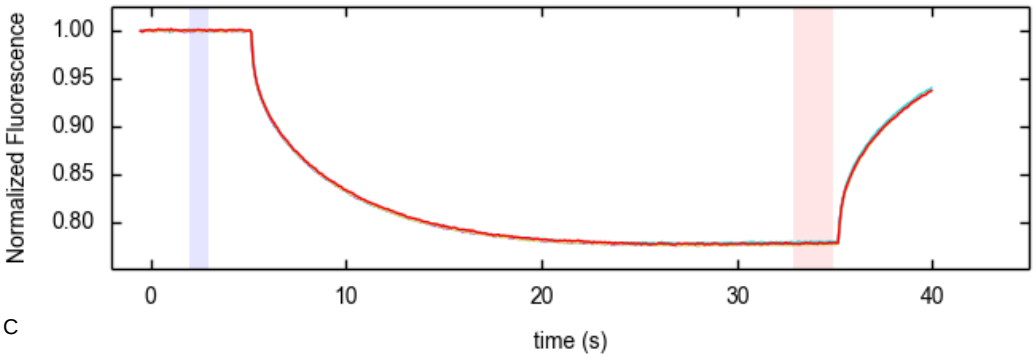
Normalized Fluorescence
1.00
0.95
0.90
0.85
0.80
0
10
20
30
40
time (s)

C

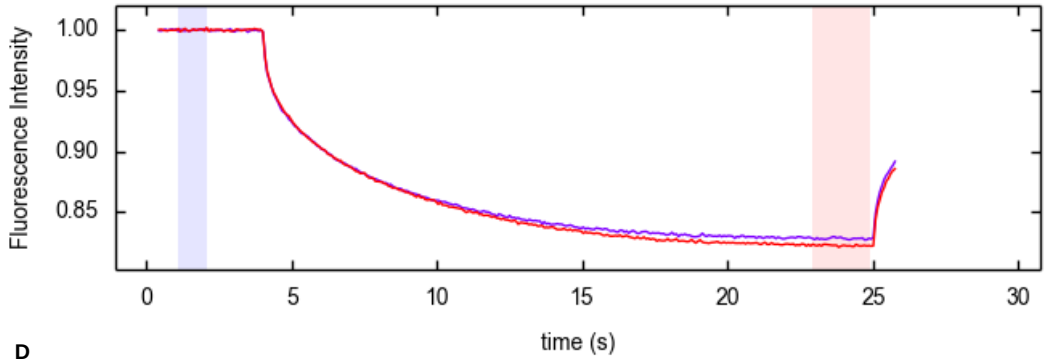
Fluorescence Intensity
1.00
0.95
0.90
0.85
0
5
10
15
20
25
30
time (s)

D

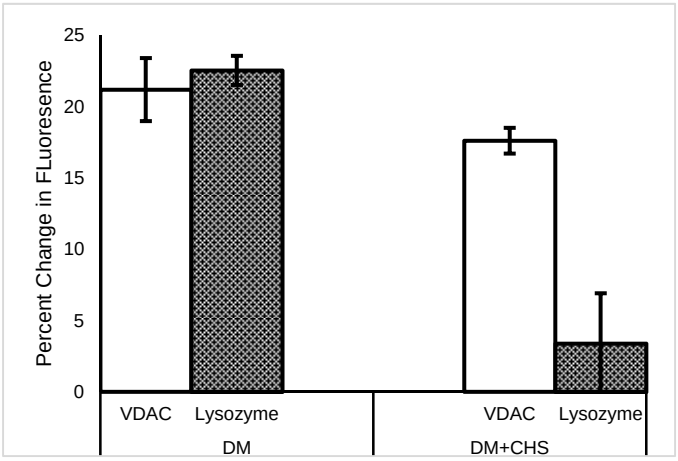
Percent Change in FLuoresence
25
20
15
10
5
0
VDAC
Lysozyme
DM
VDAC
Lysozyme
DM+CHS

Figure S2. (A) MST time traces of $VDAC^{R}$+CHS+HK-I in a 0.15% DM solution. Under these conditions the protein aggregated once the MST IR laser was activated resulting in an increase in the fluorescence over time. At high HK-I concentrations aggregates were visible in the sample capillaries after the run, the curves corresponding to capillaries with visible aggregates are indicated with a *. (B) MST time traces for screening of $VDAC^{R}$+CHS+HK-2 binding. No difference in VDAC motion due to the temperature gradient was observed between samples with and without 90μM HK-II (C)$VDAC^{R}$ MST time traces in DM solution in the absence and presence of 100 μM egg white lysozyme showing no aggregation. (D) Change in fluorescence intensity due to the addition of VDAC or egg white lysozyme in the absence and presence of CHS normalized to the fluorescence intensity of VDAC in the absence of any additional protein.

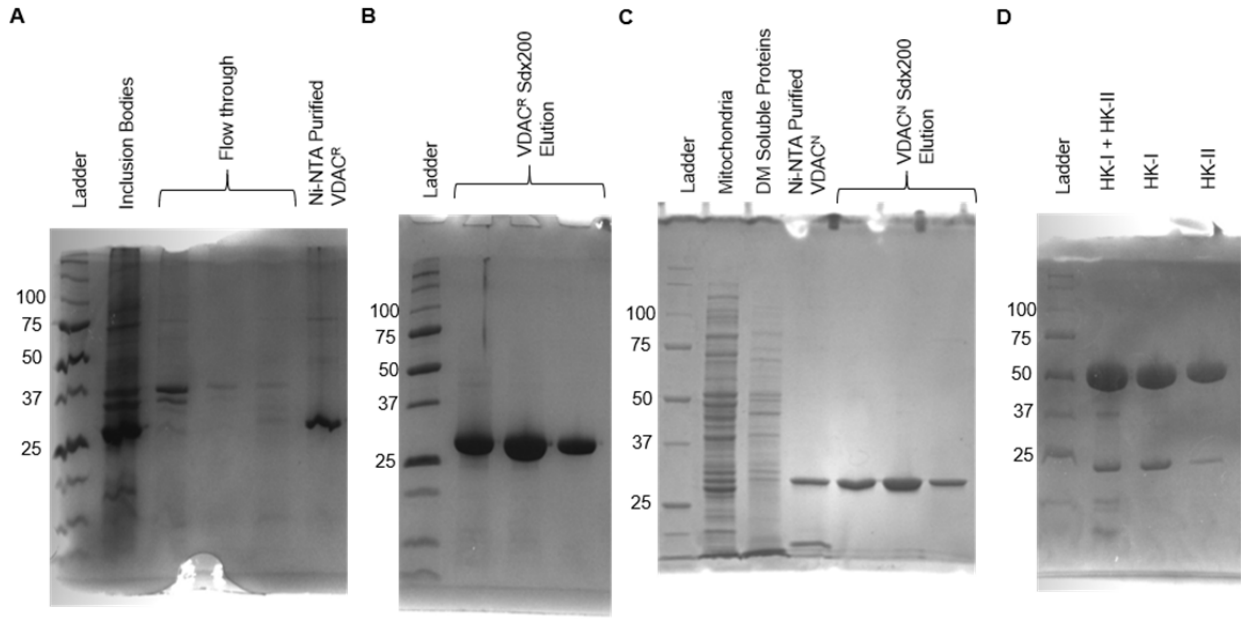

Figure S3. Full regions of interest of SDS-PAGE gels. (A) Denaturing Ni-NTA purification of VDAC^{R} from inclusion bodies (Left panel of **Fig. 1A**). (B) Refolded VDAC^{R} SEC fractions (Middle panel of **Fig. 1B**). (C) Native purification of VDAC^{N} (Right panel of **Fig. 1A**). (D) Separation of HK-I & HK-II (**Fig. 5B**). For all gels the contents of lanes are labeled directly above each lane. The M_w of relevant protein ladder bands are labeled to the right of each ladder lane.

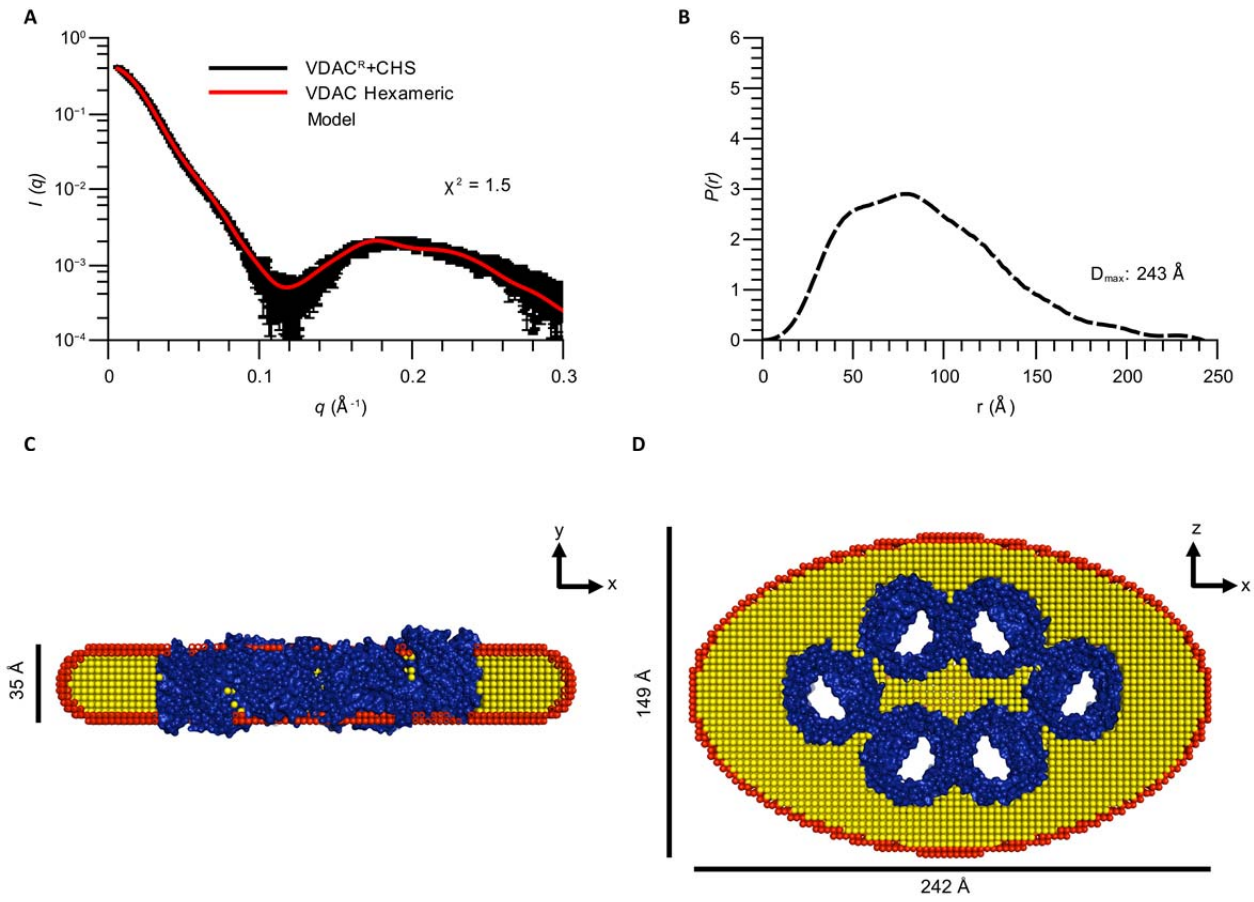

Figure S4. Anti-parallel Hexameric VDAC model fit to experimental SAXS data. (A) Experimental SAXS data (black) and calculated scattering curve of a hexameric VDAC detergent complex model (red) error bars represent standard deviation of averaged curves. The χ^2 of the fit of the model to the data is shown on the plot. (B) P(r) function calculated from experimental data of VDAC^R+CHS hexamer. Determined D_{max} value is shown on the plot. (C) Cross section of the hexameric VDAC^R+CHS model through the model with 4 of the pores visible and (D) rotated 90° around the x-axis. Dimensions of the models and the orientation relative to the axes are displayed in each panel. The protein component of the model is colored blue, the hydrophobic layer of the detergent is colored yellow and the hydrophilic layer of detergent is colored in red. Best fitting parameters of the detergent layer of the models are reported in **Table 3** and a visualization of how each parameter relates to the model can be seen in **Fig. 3**.

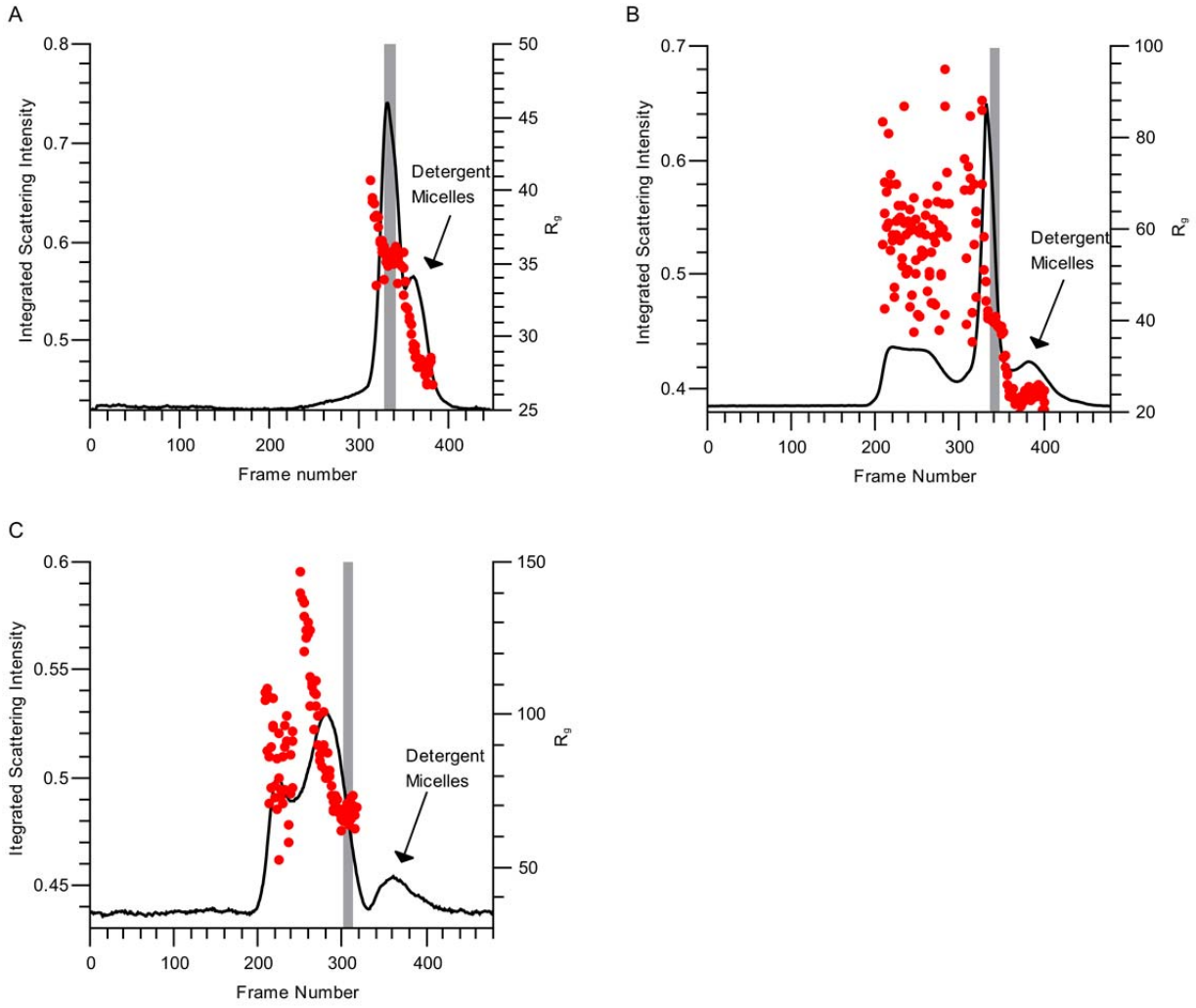

Figure S5. SEC-SAXS-Elution profiles of VDAC-detergent complexes. Elution profile of $VDAC^R$ in the absence of CHS (A), $VDAC^R$ with CHS in the column running buffer (B) and $VDAC^R$ pre-equilibrated with CHS and with CHS in the running buffer (C). In all plots the integrated scattering intensity of each frame (black lines) and R_g determined from each frame (red circles) is plotted against the frame number. The R_g of frames with integrated scattering intensities <0.03 above the buffer baseline were not determined. Peaks corresponding to excess detergent micelles in the loaded samples are indicated on each plot, these peaks were identified as detergent micelles as they were absent from the UV absorbance trace of the elution and produced identical scattering curves to detergent only samples (data not shown). The frames used in the final analysis of the VDAC-detergent complexes are indicated by the area of the plots shaded in grey.